Residual Ash Formation during Suspension-Firing of Biomass.

Effects of Residence Time and Fuel-Type

Damø, Anne Juul; Jappe Frandsen, Flemming; Jensen, Peter Arendt; Wu, Hao; Glarborg, Peter

Published in:
Proceedings of Impacts of Fuel Quality on Power Production 2014

Publication date:
2014

Residual Ash Formation during Suspension-Firing of Biomass. Effects of Residence Time and Fuel-Type.

Anne J. Damoe*; Flemming J. Frandsen; Peter A. Jensen; Hao Wu; Peter Glarborg
Department of Chemical and Biochemical Engineering, Technical University of Denmark, DK-2800 Kgs Lyngby, Denmark
*Corresponding author: E-mail: ajp@kt.dtu.dk, Tel: +45 4525 2800, Fax: +45 4588 2258

Abstract: Through 50+ years, high quality research has been conducted in order to characterize ash and deposit formation in utility boilers fired with coal, biomass and waste fractions. The basic mechanism of fly ash formation in suspension fired coal boilers is well described, documented and may even be modeled relatively precisely. Concerning fly ash formation from biomass or waste fractions, the situation is not nearly as good. Lots of data are available from campaigns where different ash fractions, including sometimes also in-situ ash, have been collected and analyzed chemically and for particle size distribution. Thus, there is a good flair of the chemistry of fly ash formed in plants fired with biomass or waste fractions, either alone, or in conjunction with coal. But data on dedicated studies of the physical size development of fly ash, are almost non-existing for biomasses and waste fractions.

The objective of this work was to generate novel and comprehensive data on the formation of residual fly ash during the initial stage (0.25 – 2.0 s) of suspension-firing of biomass (pulverized wood and straw). Combustion experiments were carried out with bio-dust (pulverized straw and wood), in an entrained flow reactor, simulating full-scale suspension-firing of biomass. By the use of a movable, cooled and quenched gas/ particle sampling probe, samples were collected at different positions along the vertical axis in the reactor, corresponding to gas residence times, varying in the range [0.25 – 2.0 s]. The collected particles were subjected to various analyses, including STA-analysis for determination of carbon/char burn-out level, light-scattering technique (Malvern Mastersizer) for determination of particle size distribution, bulk chemical analysis (ICP-EOS) for elemental composition, and, SEM/EDS analysis for investigation of particle morphology and composition. The transient release of inorganic species such as alkali metals, Cl and S from the fuel particles, was quantified by two different calculation methods.

The char burn-out level of the residual ash was found to be both time dependent and highly fuel dependent. The degree of conversion in the first 1.0 – 1.1 s of the combustion process was rather low. The physical size distribution of the residual fly ash particles evolved with residence time, towards a multi-modal particle size distribution. For both wood and straw, the particles shifted towards smaller particles with increasing time, due to char oxidation/pyrolysis, fragmentation, and ash formation. For straw, an increase in the concentration of large particles at 1.0 – 2.0 s, indicated melting and agglomeration of ash particles.

The transient release of K was massive (> 60 wt. %) for all fuels and throughout the temperature range tested. An increasing trend with increasing residence time indicated that the release of K is a time dependent process. For a Si-rich straw fuel with relatively shortage of Ca, results further indicated retaining effects on the release of K, probably due to incorporation of K into silicate

structures. The release of Cl and S was generally close to complete for all fuels, independent on residence time and temperature.

Introduction:
Replacing coal with biomass on existing suspension-fired power plants comprises an important aim in Danish Energy policy on converting the energy supply system from largely fossil-fuel based, towards a system based 100 % on renewable energy, by 2050 (the Danish Government, Our Future Energy, 2011). However, a major obstacle for the conversion from coal to biomass on existing plants, is still to manage the ash behavior in such systems. Ash-related problems, such as increased deposit formation and boiler corrosion, and deactivation of SCR (Selective Catalytic Reduction) catalyst, are among the major technical challenges reported for suspension-firing of biomass (Korbee et al., 2010; Zheng et al., 2007; Wu et al., 2011, Hansen et al., 2014).

The ash-related problems are induced by various physical and chemical transformations of the fuel during combustion. I.e. the overall/main route between a burning fuel particle in a furnace and a troublesome deposit on a heat transfer surface, can be divided into a number of consecutive steps (Korbee et al., 2010; Haynes et al., 1982; Helble, 1987; Vejahati et al., 2010):

- Conversion of the fuel by devolatilization, and char oxidation;
- Release to the gas phase of critical ash-forming elements, which for biomass being mainly K, Na, Cl, S, Ca, Si and Mg, during devolatilization, and char burnout;
- Formation of aerosol particles by nucleation and coagulation of flame-volatilized ash-forming elements during cooling of the flue gas;
- Formation and entrainment of residual ash (condensed phase ash particles) during char burnout;
- Transport of ash species i.e. gases, liquids (droplets) and solids (particles), from bulk gas to heat transfer surfaces and adhesion of these ash species to heat transfer surfaces, and;
- Build-up, sintering (consolidation) and shedding of deposits.

The physical transformations such as devolatilization, char oxidation, and fragmentation are among the most important aspects of the ash formation process in the radiant zone of a pulverized-fuel boiler. These transformations are both time-dependent and largely dependent on several fuel characteristics, and, in particular when it comes to biomass fuels, these transformations are not well described (Korbee et al., 2010). Therefore, understanding of ash formation, and being able to predict (or in the beginning, just to know) the particle size distribution, and chemical composition of the residual fly ash and the species release to the gas phase, when utilizing biomass as e.g. straw and wood for suspension-firing, is of utmost importance as a step towards preventing ash–related problems in suspension-fired biomass boilers.

Through 50+ years, research has been conducted in order to characterize ash and deposit formation in utility boilers fired with coal, biomass and waste fractions. The basic mechanism of fly ash formation in pulverized fuel (PF) fired coal boilers is well described, documented and may even be modeled relatively precisely (Haynes et al., 1982; Helble, 1987, Vejahati et al., 2010,

Flagan and Seinfeld, 1988). Concerning fly ash formation from biomass or waste fractions, the situation is not nearly as good. Lots of data are available from campaigns where different ash fractions, including sometimes also in-situ ash, have been collected and analyzed chemically (Hansen et al., 2014; Zheng et al., 2007; Wu et al., 2011; Damoe et al., 2014). So there is a good flair of the chemistry of fly ash formed in plants fired with biomass or waste fractions, either alone or in conjunction with coal (Zheng et al., 2007; Wu et al., 2011). But data from dedicated studies of the physical size development, ash species transformation and transient changes in chemical composition, of fly ash from pulverized biomass firing are limited, with Korbee and co-workers being pioneers in the field (Korbee et al., 2010; Shah et al., 2010).

Korbee et al. (2010) studied first-line ash transformations of different coal and biomass fuels under typical PF firing conditions by use of a Lab-Scale Combustion Simulator (LCS). Gas phase ash release, conversion, size reduction, and size distribution were derived alongside with changes in mineral chemical composition, for different conversion levels at 20, 90, 210, and 1300 ms of residence times, and char burn-out, devolatilization level and fragmentations were quantified. The study included wood chips, waste wood, olive residue, straw, a UK coal, and a Polish coal.

When studying the char conversion, Korbee et al. (2010) found that all the studied biomasses were to a higher degree converted than the coals, due to the comparatively lower ash contents and higher volatile matter contents. They also found that the volatilization of inorganic matter (such as K, Cl, S, Ca, Si) is also a time dependent process and not merely an instantaneous phenomenon. Most of the inorganic matter volatilization took place in the first ~200 ms of the fuel conversion process; however, the release in the last burnout stage (1300 ms) was still sizeable. Large differences were observed between fuels. Relatively low ash release was observed from wood-type fuels, reflecting their low ash contents, while high ash gas phaserelease from olive residue and straw was reflecting a higher ash content and especially a high ash volatility.

The measured mass-based particle size distribution (PSD, in wt.%) for the different fuels during char burnout revealed a significant increase in the aerosol concentration during the initial char burnout (20 and 90 ms), and it was interpretated to be a sign of burning with attritive fragmentation (Korbee et al., 2010). Furthermore, fine (1 – 10 µm size) particles concentration was found to decrease for all fuels after 90 ms, proving that that the lower size particles devolatilize and oxidize quickly as compared to larger particles. The faster conversion of the smaller char particles was observed for all fuels except a Polish coal with the highest ash content (excluded minerals). It was also found that after a certain conversion, larger (> 10 µm) particles fragmented more than the smaller particles and therefore their concentration deceased more rapidly in the later time steps, and biomass was found to be fragmenting more than coal.

The elemental distribution of particles collected with PSD was derived for each char burnout stage, and it was observed that S and Cl started to vaporize already at 20 ms in the flame itself, where the release of alkali and other minerals were still negligible. The alkali metals appeared to be vaporizing in the second time step around 90 ms (Korbee et al., 2010). In Si, or Si and Al rich fuels, such as straw and the two coals, the overall release of alkali minerals was limited (< 50 %). The release of Ca and Mg was significant in Ca and Mg-rich woody fuels, and alkali rich fuel such

as olive residue was found to be the most volatile compared to all other fuels (Korbee et al., 2010).

Shah et al. (2010) attempted to describe the complex elemental volatilization process under pulverized-fuel combustion conditions by means of simple linear correlations as a function of mineral matter compositions and their association in the char matrix. The release from 6 diverse biomass fuels and two different coals was studied experimentally in a Laboratory Scale Combustion Simulator, using similar test conditions (and fuels) as in the related study by Korbee et al. (2010). The raw release data were plotted against several chemical indices, in order to evaluate the effect of mineral matter compositions, i.e. Cl, Al, Si and S, onto the release of each individual element (K, Na, Cl, S, Ca, Mg). Linear regression lines were then plotted onto these charts, and in this way the elemental release was described as a set of linear correlations, presented for each element and for each fuel group (e.g. woody biomass, agricultural biomass/residue, coal).

In this way, Shah et al. (2010) found a close match (R^2 ~0.95) when plotting the release of K against the ratio of (K + Cl)/(Si + Al + 2S) in the fuel, implying that the higher the K and Cl levels in the fuels, the higher will be the K volatilization, but the release will be limited by Si, Al and S. Almost complete release of K was observed for clean, woody biomass with low content of Al and Si. A close match with $R^2 > 0.99$ was observed for S released against fuels levels, for various fuels (both biomass and coal) (Shah et al., 2010). Cl was found to be released completely from woody biomasses, while other fuels such as saw dust, olive residue, straw, and Polish coal, demonstrated noticeably lower release in some cases. The closest match (R^2>0.96) for a mineral matter-dependent regression was obtained when plotting the release of Cl against the ratio of Cl/(Na+K+Si+Al+2S), indicating an interconnection of the primary release mechanisms for chlorine and alkalis (. Only a partial release of Ca and Mg was observed throughout the fuel range, although with a significant release for woody biomasses containing very high share of Ca in its ash. Fuels richer in Si, such as saw dust, olive residue and straw, released much less Ca (Shah et al., 2010).

Other studied have also addressed the gas phase release of critical ash-forming elements such as alkalis, S and Cl from distinct, well-defined biomass fuels, or classes of biomass fuels, but primarily during fixed-bed/grate-firing conditions (Knudsen, 2004; Knudsen et al., 2004, 2005; van Lith 2005; van Lith et al., 2006, 2008; Frandsen et al., 2007). These studies generally agree that Cl enhances K vaporization, while Si reduces K volatility by incorporating K into silicate structures, and it has been suggested that the release of KCl in principle may overrule all retention effects (Knudsen, 2004; Novakovic et al., 2010). Knudsen (2004) found from lab scale release experiments with annual biomass fuels that it was possible to drive all K into the gas phase (as KCl or $(KCl)_2$), by addition of HCl to the fuel sample, at temperatures above 900 ^oC. On the other hand, excess levels of Si and Al may retain the release of K, due to incorporation into stable potassium-aluminium-silicates (Shah et al., 2010; Knudsen, 2004, Knudsen et al., 2004).

Concerning the release of S and Cl, it is also generally agreed that overall S is almost completely released to the gas phase as SO_2 while Cl is released almost completely as HCl or CH_3Cl (Saleh et

al., 2014) already at low temperatures. Further, SO_2 may react with alkali chlorides to form alkali sulfates, if the fuel S/Cl molar ratio is high, or may react with Ca and Mg to form sulfates at < 1450 ^oC. S and aluminosilicates competes for alkalis. High T favors alkalis alumino-silicates over sulfate formation (Shah et al., 2010). Cl effect on alkali release is pronounced (Knudsen, 2004; Shah et al., 2010).

Few studies address the effects of Ca and Mg on the behavior of Cl and alkali metals. Alumino-silicates are more likely to react with Ca and Mg than with alkalis. Therefore, it is expected that higher levels of Ca will cause more alkalis to remain as gaseous alkali chlorides, sulfates or (hydr)oxides even at high temperatures (Shah et al., 2010; Knudsen, 2004). This effect has been confirmed by means of release experiments on synthetic samples of K-Ca-Si mixtures, by Novakovic et al. (2010).

Despite the numerous studies addressing the gas phase release of ash forming elements from various biomass fuels, attempts to make a more general model for prediction of the release, which is applicable for a wider range of fuels (not to mention different combustion technologies), have been very scarce (Knudsen, 2004; Knudsen et al., 2004; Shah et al., 2010). Knudsen and co-workers (2004) studied the release from annual biomass during fixed-bed combustion conditions and proposed simple, linear correlations for the release of K, Cl and S from annual biomass fuels, based solely on the inorganic composition of the fuels. The K release was found to depend in particular on the Cl and Si-content in the fuel, and thus the fuels were initially categorized into two different categories, i.e. *Si-lean fuels* (K/Si molar ratio > 2), and *Si-rich fuels* (K/Si molar ratio < 2), exhibiting different release behavior. Following, release estimates for K including simple, linear expressions for min and max release, based on Cl/K and (Ca+K)/ Si molar ratios were derived. Importantly (as opposed to e.g. the study by Shah et al., 2010), Knudsen also incorporated the liberating effect of a high Ca content on the release of K from Si-rich fuels, in the expressions.

Objectives of present work:

The objectives of the present work are to generate implicit comprehensive data on the formation of fly ash from suspension-firing of biomass. The main subjects investigated include 1) Studies of ash transformations such changes in particle size distribution and chemical composition, and release of inorganic elements, as a function of residence time; 2) Influence of fuel type and composition on fly ash properties. This is done by conducting combustion experiments with bio-dust in an entrained flow reactor. With the data obtained, we aim at complementing and extending significantly the limited data available from the few previous, dedicated studies in the field (Korbee et al., 2010; Shah et al., 2010). It should be noticed that our study differs significantly from the studies by Korbee and co-workers on several parameters, most importantly the experimental set-up (and fuels) used, the conversion levels (residence times) studied, and the assumptions we use for quantifying the release, as described in details in the experimental section.

Experimental:

The DTU solid fuel entrained flow reactor:

The experimental set-up consists of an electrically heated solid fuel entrained flow reactor (EFR) and additional support equipment, as shown in Figure 1. The reactor system basically consists of three parts: A fuel feeding and gas preheater section in the top, the reactor section itself, consisting of a 2 m long ceramic tube with an inner diameter of 8 cm, lined with 7 heating elements (T max = 1475 ^{o}C), and, a water cooled bottom chamber. The bottom chamber has a hole in the bottom for insertion of a gas/particle extraction probe, and several flanged openings in the side, of which one is connected to the exhaust system. The EFR has previously been used to study ash behavior during e.g. co-firing of coal and straw (Zheng et al., 2007), and co-firing of coal and solid recovered fuel (Wu et al., 2011). For the present experiments, the setup was used to combust bio-dust (various pulverized straw and wood fuels, see Table 1) and hence resembled biomass combustion in a pulverized fuel furnace. Furthermore, the setup was equipped with a movable gas/particle sampling probe, allowing collection of gas and particle samples at different gas residence times from ~0.25 – ~2 s.

The gas/particle sampling system:

A movable gas/particle sampling probe has been designed to extract and quench a fraction of the flue gas/particles, at different gas residence times (ranging from ~0.25 to ~2 s) in the reactor. The movable sampling probe is water-cooled and thermo stated to 60 ^{o}C to ensure that flue-gas water do not condensate in the probe, and the gas and particle sample, which can be extracted at (close to) isokinetic sampling conditions, at any position along the reactor vertical axis (i.e. at different gas residence times), is quenched with N_2 directly in the probe tip, in order to force fast nucleation of vaporized species. The quench N_2 flow and suction flow can be adjusted in order to obtain isokinetic sampling conditions. The gas composition (O_2, CO_2, CO, NO, SO_2) of the quenched flue gas from the probe, and the raw gas from the reactor outlet, is monitored continuously by standard gas analyzers, and the difference in CO_2 concentrations is used to determine the actual quench dilution ratio.

The quenched and cooled sample gas from the probe is led to a particle sampling panel (see Figure 1), where it passes first through a cyclone which separates out the coarse fly ash fraction (cut-off diameter ~1.5 µm). From the cyclone, (a fraction of) the flue gas is directed through a 0.1 µm PE filter where the sub-micron aerosol particles are collected. The temperature in the extraction line, from the outlet of the probe and through the cyclone and aerosol filter, is maintained at ~80 ^{o}C to ensure that the flue gas temperature is above the water dew point. We assume that the fraction of particles captured in the aerosol filter (< ~1.5 µm) represents the fraction of the ash that has been released/volatilized during the combustion (similar to the assumption used by Korbee et al., 2010). The particles separated in the cyclone may contain both coarse fly ash particles representing the residual (non-volatilized) fly ash according to the definition by Korbee et al., 2010, in addition to a certain fraction of aerosol particles attached to the surface of larger fly ash particles, or present agglomerates larger than ~1.5 µm. The latter (the fraction of (agglomerated/attached) aerosol particles trapped in the cyclone together with the larger residual fly ash particles), may be quantified by determining the fraction of water-

soluble K, Cl and S, as the fraction of water soluble K in fly ash provides information on the fraction of K that appears as salts (KCl and K_2SO_4) (Zheng et al., 2007).

A schematic overview of the mass flows and characterization routes (residual vs. released ash) for the measurements is shown in Figure 2.

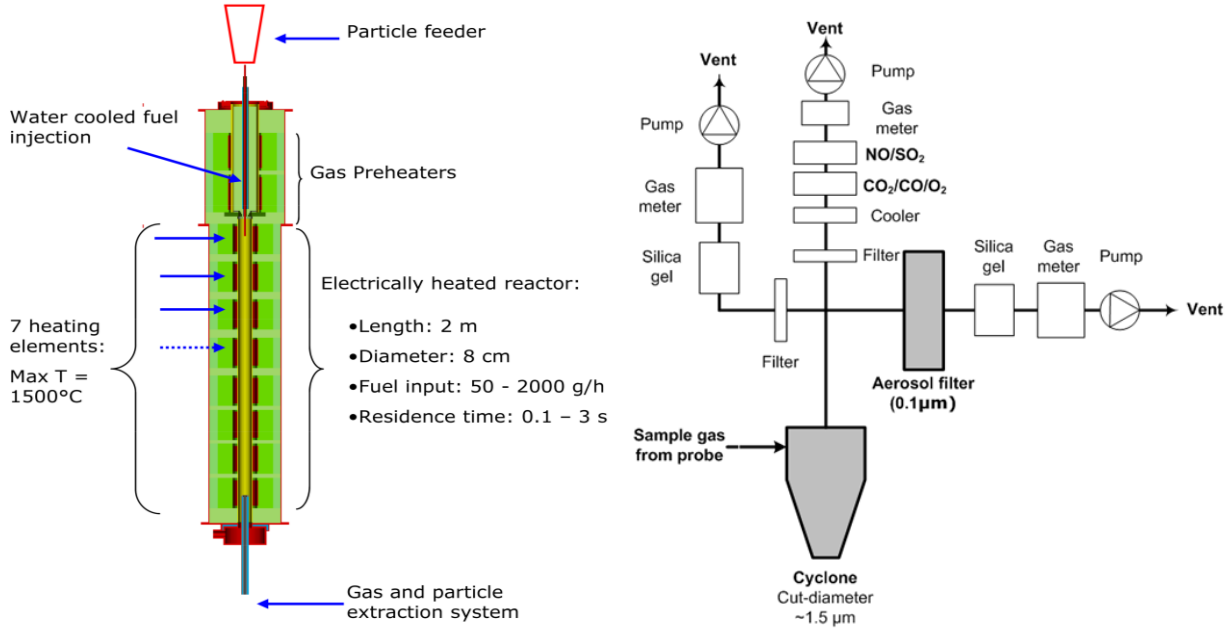

Figure 1: The DTU solid fuel entrained flow reactor (left) and the gas/particle sampling system (right)

<u>Mass balances and quantification of release:</u>
After each experiment, the ash particles collected in the cyclone and aerosol filter are weighed and saved for analyses. Additionally three ash material samples are recovered and weighed: Ash deposited in the sample line between the probe and the cyclone ("coarse ash in hoses/pipes") (fraction M_3 on Figure 2), material deposited on the probe top ("coarse ash on probe top") (fraction M_2 on Figure 2), and condensed salts deposited at the quench gas inlet inside the probe tip ("fine (condensed) ash in probe tip") (fraction M_5 on figure 2). M_4 and M_6 (not collected ash/aerosol) represent "not recovered ash fractions" and may include losses due to e.g. accumulation/deposition on reactor wall, or losses in the sampling lines.

For ash and elemental mass balance calculations, the following is assumed for each experiment:

a) The fraction of organic matter in the ash collected in hoses/pipes (M_3) is the same as in the cyclone ash (M_{cy}), while the fraction of organic matter in the aerosol filter ash (M_{fi}), in the condensed salts in probe tip (M_5), and in the deposit on the probe top (M_2) is assumed to be zero

b) Ash collected on the probe top (M_2) and ash collected in hoses/pipes (M_3) have an ash composition similar to the cyclone ash (after correcting for organic matter content according to assumption a))
c) Condensed salts inside the probe tip (M_5) has a composition similar to the aerosols collected in the filter
d) All elements are to an equal degree deposited in the reactor, and to an equal degree collected by the probe

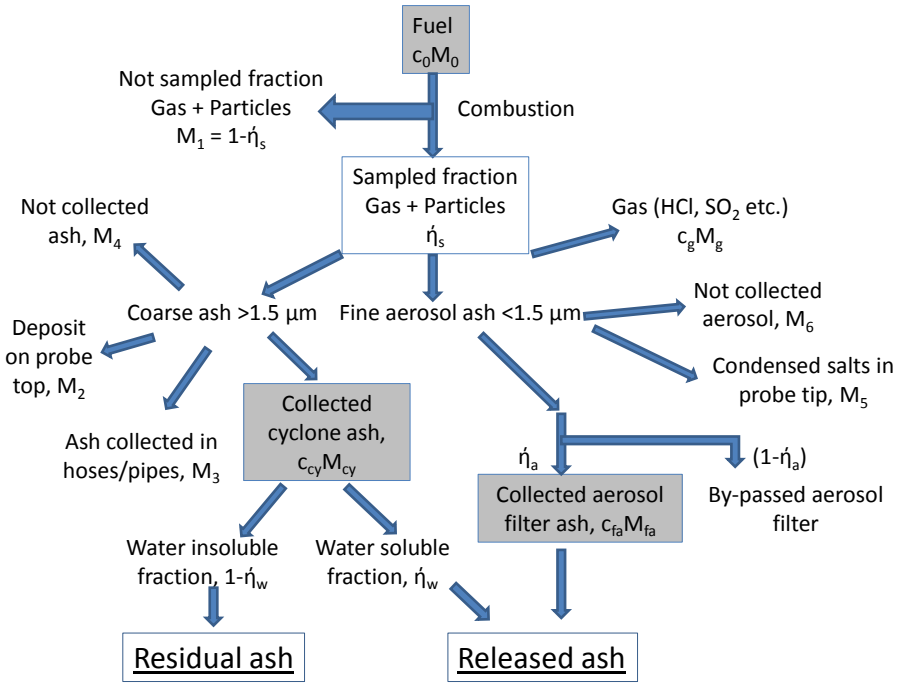

Figure 2. Schematic overview of the mass flows and characterization routes (residual vs. released ash) for the measurements. $ή_s$ is the sampling efficiency (i.e. the fraction of gas/particles extracted by the probe), $ή_a$ is the fraction of the sample gas that is directed through the aerosol filter, and $ή_w$ is the fraction of water-soluble K, Cl or S determined in the cyclone ash. c_i is the mass fraction of the ash, or an element present in the ash, (e.g. mg/g, or wt%) obtained at location *j*, M*j* is the mass (g) of the material obtained at location *j* (e.g. ash collected in the cyclone, M_{cy}).

According to the characterization route in Figure 2, and assumption a) above, the ash mass balance recovery (% recovery, not to be confused with the sampling efficiency $ή_s$) is then defined as:

$$(1) \quad ή_{recov,ash} = \frac{M_{ash,out}}{M_{ash,in}} * 100\% = \frac{(1 - c_{org,cy})(M_{cy} + M_3) + M_{fa}\frac{1}{ή_a} + M_2 + M_5}{(1 - c_{org,0})M_0 ή_s}$$

Where $c_{org,cy}$ is the mass fraction of organic matter measured in the material collected in the c**y**clone (e.g. 85 wt.%), and $c_{org,o}$ is the fraction of organic matter in the fuel (e.g. 99 wt.% for wood).

Further, when using assumption b), c) and d), the elemental recovery becomes:

$$(2) \quad \acute{\eta}_{recov,element} = \frac{M_{element,out}}{M_{element,in}} * 100\%$$

$$= \frac{c_{cy}\left(M_{cy} + M_3 + M_2\frac{1}{(1-c_{org,cy})}\right) + c_{fa}\left((M_5 + M_{fa}\frac{1}{\acute{\eta}_a}\right) + c_g M_g}{c_0 M_0 \acute{\eta}_s} * 100\%$$

And the elemental release, in % of $M_{element,out}$ ("recovered" basis) in the experiment, is defined as:

$$(3) \quad \acute{\eta}_{rel} = \frac{c_{cy}\left(M_{cy} + M_3 + M_2\frac{1}{(1-c_{org,cy})}\right)\acute{\eta}_w + c_{fa}(M_5 + M_{fa}\frac{1}{\acute{\eta}_a}) + c_g M_g}{c_{cy}\left(M_{cy} + M_3 + M_2\frac{1}{(1-c_{org,cy})}\right) + c_{fa}\left((M_5 + M_{fa}\frac{1}{\acute{\eta}_a}\right) + c_g M_g}$$

Where c_{cy} is the mass concentration (mg/kg, or wt.%) of the element determined in the material collected in the cyclone, c_{fa} is the concentration of the element determined in the aerosol filter ash, c_g is the concentration of the element determined in the flue gas (applicable for S only (as SO_2)), and c_0 is the concentration of the element in the fuel.

The elemental release quantification method outlined in equation (3) is hereafter termed *Release Quantification Method 1*.

An alternative quantification method, hereafter termed *Release Quantification Method 2,* is also introduced, based on a slightly modified version of the release quantification method suggested by Korbee and co-workers (Korbee et al., 2010; Shah et al., 2010). The release using *Method 2* is calculated as *the difference between the amount of inorganic matter in the fuel (corrected for experimental ash recovery $\acute{\eta}_{recov(Ca,Si)}$) and the amount of inorganic matter left over in the (non water soluble) coarse ash fractions after (partial) conversion:*

$$(4) \quad \acute{\eta}_{rel(method\ 2)} = \frac{c_0 M_0 \acute{\eta}_{recov,(Ca,Si)} - c_{cy}\left(M_{cy} + M_3 + M_2\frac{1}{(1-c_{org,cy})}\right)(1-\acute{\eta}_w)}{c_0 M_0 \acute{\eta}_{recov,(Ca,Si)}}$$

Where the experimental recovery $\acute{\eta}_{recov(Ca,Si)}$ (ash mass balance) for each experiment is calculated by assuming Ca and/or Si being stable "marker" elements exhibiting zero release (i.e. Ca and Si are used as ash tracers; assuming that these elements should be transferred 100 % to the coarse ash fractions):

$$(5) \quad \acute{\eta}_{recov,(Ca,Si)} = \frac{M_{(Ca,Si),out}}{M_{(Ca,Si),in}} * 100\%$$

As compared to the method used by Korbee and co-workers, we have modified the *Method 2* to include also the fraction of water-soluble K, Cl and S in the cyclone ash ($\acute{\eta}_w$) in the "released" part of the ash, as seen from equation (4).

The major advantage of *quantification method 1* is that it is comprehensive in including all (5) collected ash fractions (in addition to the flue gas composition when applicable) in the ash and elemental mass balance calculations, as specified in Figure 2 and equation (1) – (3). Following, with this method we obtain experimental (ash) mass balances that can be closed within >43 % recovery in the present experiments, as indicated in Table 3 in the results section. This is considered acceptable, as previous experiences with the EFR indicate that the experimental ash recovery is often not greater than 40 - 80 % and deviates considerably in different experiments, due to deposition on reactor wall and other surfaces (Wu et al., 2011; Zheng et al., 2007).

On the other hand, the ash mass balance (and hence the recovery) calculations for each experiment using *method 1* prerequisite accurate input data for both sampling efficiency in the probe (which is calculated from the CO_2 dilution ratio), and the content of unburnt organic matter in the collected ash fractions (which is determined by STA analysis). Another important limitation of quantification method 1 is on the analytical determination of specific elements especially in the "released" (aerosol filter) ash fractions, where wet chemical analysis is not always possible, due to a limited amount of sample mass available.

The major advantage of *quantification method 2* is that it is simple and with fewer uncertainties as compared to method 1. The major drawback is that with this calculation method, the actual ash and elemental mass balances are not closed.

A general limitation for the quantification of the release of specific elements (for both methods) is that the concentration of the element in certain ash fractions may be close to, or even below, the detection limit of the chemical analysis (due for S, Si, Cl, Na).

Fuels utilized:

Two different straw fuels and two woody biomasses were used in the EFR experiments, fuel analyses are provided in Table 1. The two straw fuels were characterized by high contents of K, Si and Cl, and an ash content of > 4 wt%, while the woody fuels were dominated by Ca, K and Si, a low ash content ≤ 1 wt%, and only traces of Cl. All fuels were milled/pulverized, prior to use in the EFR, in order to reach a to a particle size < ~700 µm.

Experimental matrix:

An experimental matrix, testing two different reactor temperatures, and three different sampling positions/gas residence times, respectively, was set up, as seen in Table 2. The three sample probe positions corresponded to gas residence times in the range 0.25 to 2.0 seconds, depending on the reactor temperature (see details in Table 2). In order to obtain an excess air ratio around 1.5 (corresponding to an exit flue gas O_2 level of approximately 6.5 vol. %), the inlet air flow rates in the study were 30 nL/min, and particle feed rates were in the order of 0.2 - 0.3 kg/h. The duration of an experiment was limited by the pressure drop in the particle sampling system, i.e.

the experiment continued as long a constant flow could be obtained through the aerosol filter (≤ 35 min in case of straw fuels, ≤ 90 min in case of wood fuels). Steady-state conditions (i.e. stable flow and temperature) were assumed.

Table 1: Fuel analysis.

		Fuel 1 "Straw"	Fuel 2 "BRISK SP" (Straw)	Fuel 3 "Wood"	Fuel 4 "BRISK WP" (Wood)
Water	%, as recieved	7.4	12.5	9.7	7.9
Ash	%, dry basis	4.2	4.6	1	0.4
Volatiles	%, dry basis	75.9	76.5	83.3	84.6
Higher heating value	MJ/kg, dry basis	18.92	18.97	20.22	20.36
Lower heating value	MJ/kg, dry basis	17.65	17.66	18.87	19.02
C	%, dry basis	46.9	48.7	50.8	52.2
H	%, dry basis	6	6	6.2	
N	%, dry basis	0.56		0.17	
S	%, dry basis	0.12	0.08	0.013	0.005
Cl	%, dry basis	0.65	0.18	0.004	0.004
Al	%, dry basis	0.044	0.023	0.0126	0.0058
Ca	%, dry basis	0.230	0.360	0.228	0.085
Fe	%, dry basis	0.041	0.018	0.0081	0.0041
K	%, dry basis	1,4	0.8	0.0926	0.0410
Mg	%, dry basis	0.096	0.063	0.035	0.011
Na	%, dry basis	0.023	0.028	0.0028	0.0011
P	%, dry basis	0.091	0.075	0.0122	0.0041
Si	%, dry basis	0.39	1.10	0.100	0.020
Ti	%, dry basis	0.0042	0.0017	0.00086	0.0005
Cl/K	mol/mol	0.51	0.25	0.05	0.11
S/K	mol/mol	0.10	0.12	0.17	0.15
K/Si	mol/mol	2.58	0.52	0.67	1.47
Ca/Si	mol/mol	0.41	0.23	1.60	2.98

Characterization of ash particles:

Selected samples of the collected ("residual" and "released") ash particles were subjected to the analytical methods outlined below:

Characterization of residual (cyclone) ash particles by STA analysis. Simultaneous Thermal Analysis (STA) was employed to determine the content of organic matter of the cyclone fly ash. 5 mg of cyclone ash sample was loaded in a platinum (straw ashes) or Alumina (wood ashes) crucible and heated at 10 °C/min (in N_2 and N_2+O_2 atmosphere) to the final setting temperature in a thermogravimetric apparatus (Netzsch STA-449F1). The applied temperature program and gas environment can be found in Qin et al. (2012). The content of organic matter in the cyclone ashes ($c_{org,cy}$, according to the definition in equation (1)), as determined by the STA analysis, was then used to estimate the *char burn-out level*, as determined by the ash tracer method outlined in equation (6) (Wu et al., 2011):

$$B = \left[1 - \frac{A_0}{100 - A_0} \times \frac{100 - A_i}{A_i}\right] \times 100 \qquad (6)$$

Table 2: Experimental matrix for combustion experiments in the EFR.

EFR experiments:	Temperature settings:		Fuel feed rate	Gas flow settings (l[N]/min)				Gas residence time
Fuel ID & Exp. short name	Pre-heater temp.	Reactor temp.	kg/h	N_2 quench	Main air	Feeder air	Purge air	(s)
Straw 1200 2s	1100	1200	0.295	5.48	15	10	5	2
Straw 1200 1.1s	1100	1200	0.295	5.48	15	10	5	1.1
Straw 1200 0.28s	1100	1200	0.295	5.48	15	10	5	0.28
Straw 1400 1.7s	1100	1400	0.295	5.48	15	10	5	1.7
Straw 1400 1s	1100	1400	0.295	5.48	15	10	5	1
Straw 1400 0.25s	1100	1400	0.295	5.48	15	10	5	0.25
BRISK SP 1400 1.7s	1100	1400	0.295	5.48	15	10	5	1.7
BRISK SP 1400 1s	1100	1400	0.295	5.48	15	10	5	1
Wood 1200 2s	1100	1200	0.267	5.48	15	10	5	2
Wood 1200 1.1s	1100	1200	0.267	5.48	15	10	5	1.1
Wood 1400 1.7s	1100	1400	0.267	5.48	15	10	5	1.7
Wood 1400 1s	1100	1400	0.267	5.48	15	10	5	1
Wood 1400 0.25s	1100	1400	0.267	5.48	15	10	5	0.25
BRISK WP 1400 1.7s	1100	1400	0.267	5.48	15	10	5	1.7
BRISK WP 1400 1s	1100	1400	0.267	5.48	15	10	5	1

Where B (%) is the char burn-out, A_0 (wt.%) is the ash content of the dry fuel (from table 1), and A_i (wt.%) is the mean ash content in the cyclone ash ($1\text{-}c_{org,cy}$).

Particle size distribution of residual fly ash by laser diffraction. The particle size distribution of the pulverized fuels and residual (cyclone) ashes, respectively, was determined by light scatter technique (laser diffraction, Malvern Mastersizer), in order to investigate the physical particle size development of the residual fly ash as a function of residence time. As the method requires quite large amounts of sample (generally > 100 mg), only a limited amount of cyclone ash samples from Straw and Wood combustion experiments, respectively, could be analyzed.

Wet chemical analysis of selected coarse and fine ash fractions (cyclone, aerosol filter ash, hoses/pipes ash). The chemical composition of selected coarse and fine ash fractions were determined by wet chemical analyses (pressurized acid digestion of the ash samples and subsequent determination of various elements by ICP-OES analysis). The elements determined included: Ca, Cl, K, Mg, Na, P, S, Si, and water soluble fractions of Cl, K, and S. The wet chemical

analyses were made by FORCE Technology, an external accredited laboratory. The results obtained were used as input for e.g. elemental mass balance calculations, and quantification of the release. However, as wet chemical analysis requires sample masses larger than approximately 50 mg, it was not always possible to analyze all relevant ash fractions, especially not all aerosol fractions.

SEM/EDX on selected samples from cyclone, aerosol filter and hoses/pipes: Scanning Electron Microscopy / Energy Dispersive X-ray analysis was employed to study the morphology (structure, size, shape) and (semi-quantitative) elemental composition of various coarse and fine ash fractions. The semi-quantitative elemental composition analysis by EDS was used as a supplement to the wet chemical analysis, as this was not always applicable (e.g. on aerosol particle fractions).

Results and discussiion:

Char burn-out:

The char burn-out level as function of gas residence time for the cyclone ashes obtained in the different experiments, is illustrated in Figure 3.

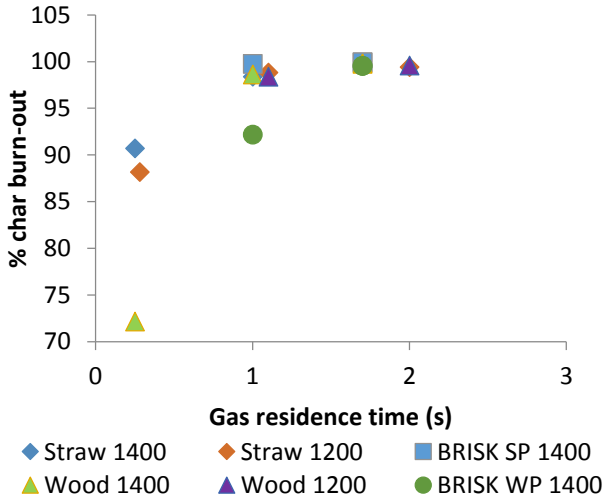

Figure 3: % char burn-out as function of gas residence time, as determined by the ash tracer method.

From Figure 3 it is seen that the char burn-out level is time and fuel dependent, while less dependent on temperature. The two wood fuels ("Wood" and "BRISK WP" reaches lower overall degree of conversation in the first ~1 s of the combustion process, as compared to the two straw fuels ("Straw" and "BRISK SP"). However, it should be noticed that the different fuels may not be directly comparable, as e.g. the particle size and shapes may vary significantly.

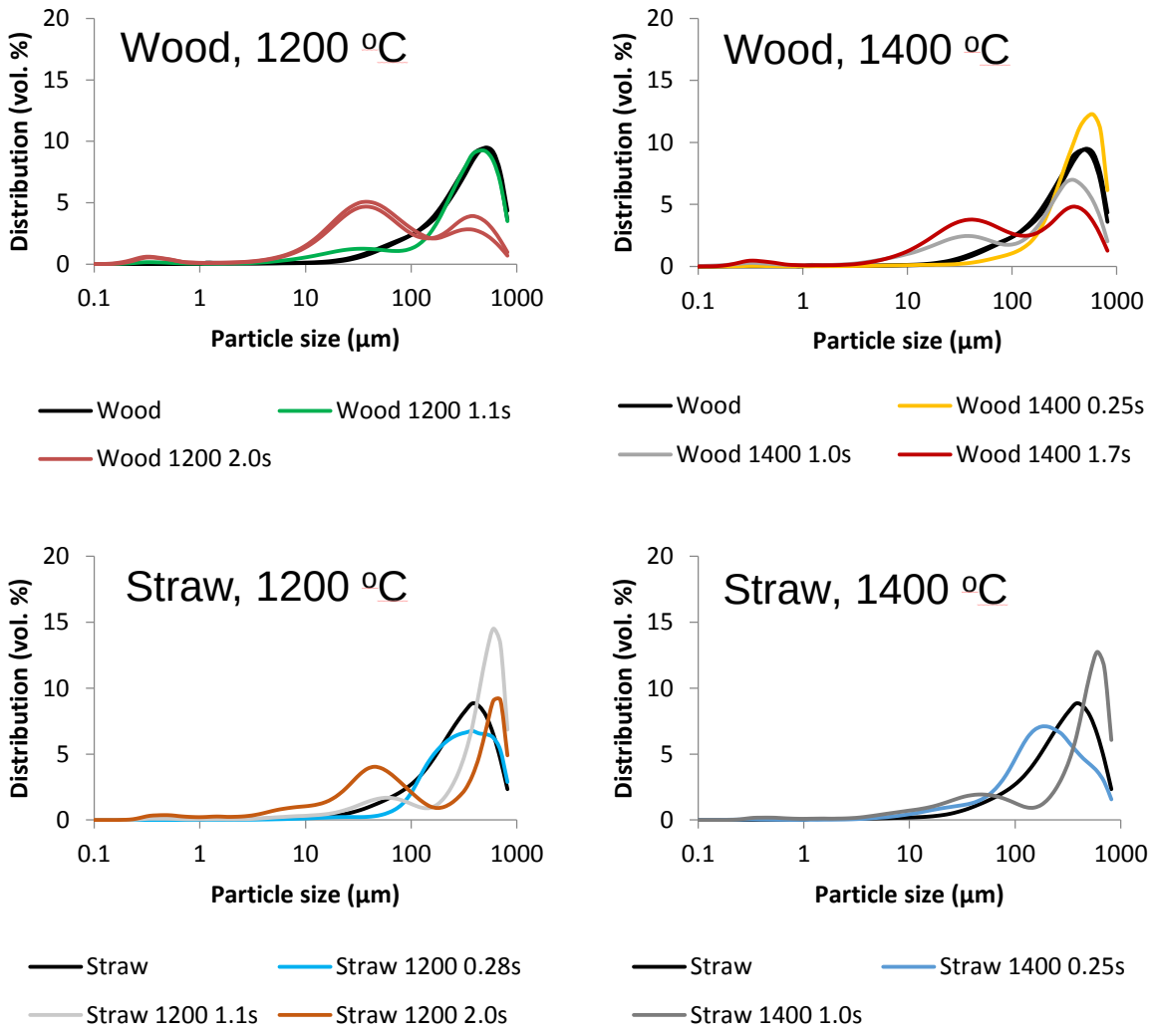

Figure 4: Particle size distribution of raw fuel and the residual (cyclone) fly ash collected at different residence times.

Physical particle size development of residual fly ash:

The particle size distribution for the raw fuel and the residual (cyclone) fly ash collected at different gas residence times, is depicted for a number of Straw and Wood experiments in Figure 4. A comparison of the corresponding fuel and cyclone ash properties is provided in Table 3, and some SEM pictures illustrating the morphology and particle size of the cyclone ash particles are provided in Figure 5 and 6.

Table 3: Comparison of fuel and cyclone ash properties for the experiments shown in Figure 4. The experimental ash balances (% recovery, $\acute{\eta}_{recov,ash}$ as defined in equation (1)), obtained in the different experiments, are also provided.

		Wood fuel	**Wood Cyclone ash**					**Straw fuel**	**Straw Cyclone ash**					
		Wood (fuel)	1200 C/1.1s	1200 C/2.0s	1400 C/0.25s	1400 C/1s	1400 C/1.7s	Straw (fuel)	1200 C/0.28s	1200 C/1.1s	1200 C/2.0s	1400 C/0.25s	1400 C/1s	1400 C/1.7s
Ca	Wt%, db	0.23	12.0	25.0	0.80	16.0	23.0	0.23	1.10	8.30	10.0	2.50	8.00	11.0
K	Wt%, db	0.09	1.40	2.10	0.30	2.60	3.10	1.40	5.80	17.1	18.0	9.20	16.0	15.0
Mg	Wt%, db	0.04	1.60	3.50	0.12	2.30	3.30	0.10	0.49	3.20	3.70	0.99	3.20	1.70
Na	Wt%, db	0.00	0.07	0.12	0.05	0.10	0.13	0.02	0.10	0.29	0.34	0.13	0.25	4.40
P	Wt%, db	0.01	0.60	1.40	0.43	0.82	1.20	0.09	0.43	2.50	3.00	0.75	2.30	0.22
Si	Wt%, db	0.10	4.40	9.00	0.50	6.90	12.0	0.39	2.10	12.0	13.0	4.10	11.0	18.0
S	Wt%, db	0.01	0.21	0.30	0.05	0.32	0.33	0.12	0.41	0.94	0.72	0.74	1.30	0.82
Cl	Wt %, db	0.004	0.12	0.32	0.05	0.27	0.22	0.65	1.90	8.00	8.80	3.80	7.60	7.00
Organic content	Wt%, db	99.0	61.5	30.0	96.5	58.0	19.0	95.8	73.0	21.0	12.0	68.0	27.0	10.0
Ash content	Wt%, db	1.00	38.5	70.0	3.50	42.0	81.0	4.20	27.0	79.0	88.0	32.0	73.0	90.0
Cl, water soluble	Wt%, db		0.12	0.33			0.23		2.20	8.30	9.20			7.50
K, water soluble	Wt%, db		1.00	1.50			2.20		6.40	14.4	14.9			11.0
S, water soluble	Wt%, db		0.19	0.21			0.30		0.37	0.92	0.72			0.82
Ash balance (method 1)	% ash recovery in exp.		57	48	98	48	62		85	80	45	75	49	43

Wood, 1400 °C:

The size distribution of the original fuel presents a broad peak in the size interval 10 – 700 µm, with maximum at ~500 µm. During combustion, the physical size distribution of the char/ash evolves with residence time, towards a multi-modal size distribution. At the initial 0.25 s of conversion, the wood ash particles concentration in the size interval 10 – 240 µm is decreased, while a relative increase in the concentration of larger particles (240 – 700 µm) is seen. This indicates that lower fuel particle sizes convert (devolatilize and oxidize) quickly compared to larger particles, in consistence with the observations by Korbee et al. (2010). Table 3 reveals that the fraction of organic matter (volatiles + fixed carbon) in the wood cyclone ash at 0.25s residence time is still very significant (96.5 wt. %), proving that the fuel is only partially converted and suggesting that the larger particles peak consists primarily of char particles. The char structures

appear in the SEM (backscattered) electron images as larger (10 – >500 µm), quite dark, irregular particles with a porous structure (Figure 5 a).

At ≥ 1.0s residence time, the concentration of the larger particles above 240 µm is fading with increased conversion of the char, while a new peak with maximum around 30 – 50 µm develops. SEM investigations of the 1.0s and 1.7s wood ash (Figure 5 b) and c)) reveal that the particles in the intermediate size interval from around 10 – 100 µm consist of spherical fly ash particles rich in Ca and Si, with various content of K, in addition to irregular ash and char particles. The surface of the (receding) char particles may be irregular or smoothed/melted, and more or less covered with smaller ash/aerosol particles. This suggests fragmentation of char and mineral inclusions as well as melting and coalescence of ash droplets as primary formation mechanisms of the intermediate particle size fraction. Table 3 confirms an increasing concentration of Ca and Si in the cyclone ashes with increasing residence time, while the fraction of combustible matter is decreasing, although it is still significant even after 1.7s residence time (19 wt. %).

In addition to the two peak described above, Figure 4 reveals a third, submicron (vaporization-mode) peak in the size interval 0,1 – 1 µm, reflecting the presence of aerosol particles originating mainly from homogeneous nucleation and subsequent coagulation of flame-volatilized inorganic species. The appearance of this vaporization peak in the cyclone ash is probably an artifact of the PSD measuring method. During PSD measurements at the Malvern Mastersizer, the samples were dispersed in ethanol, and the results probably reflects that aerosol particles originally present as agglomerates, or attached to the surface of larger fly ash particles (e.g. Figure 5 c)), have been re-dispersed.

The above described tendencies for wood cyclone ash converted at 1400 °C seem to be consistent for wood cyclone ash converted at 1200 °C.

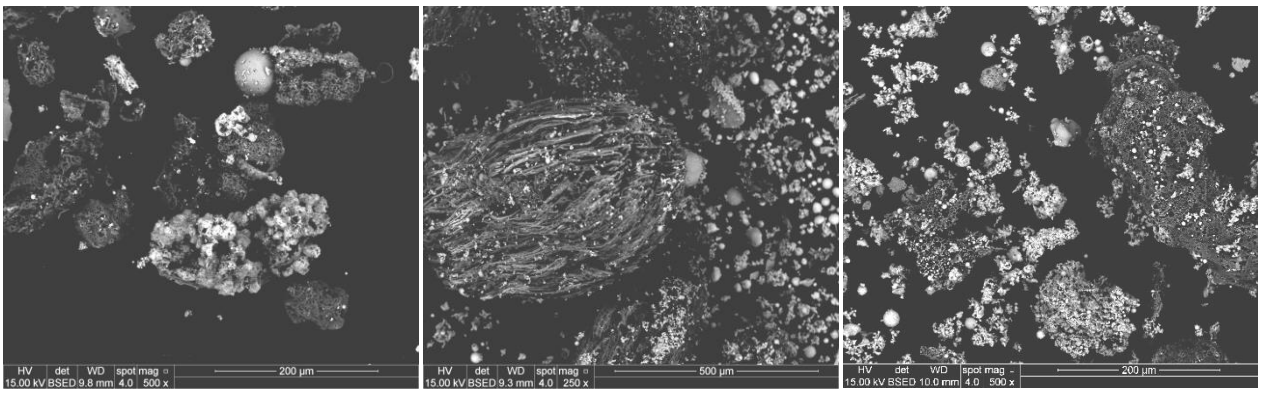

Figure 5. SEM images of wood cyclone ashes (1400 °C) obtained at different levels of conversion. From left: a) Wood 1400 0.25s. b) Wood 1400 1.0s. c) Wood 1400 1.7s.

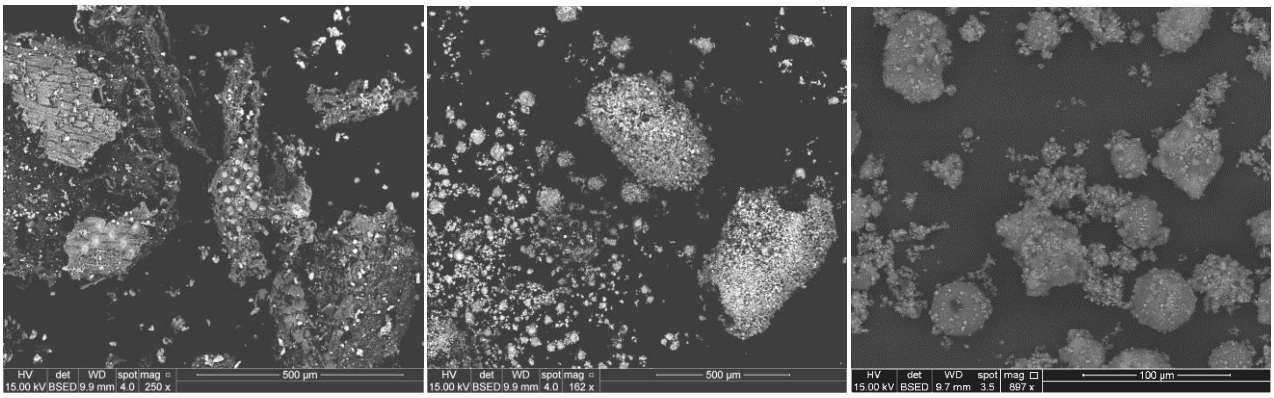

Figure 6. SEM images of straw cyclone ashes (1400 °C) obtained at different levels of conversion. From left: a) Straw 1400 0.25s. b) Straw 1400 1.0s. c): Straw 1400 1.7s.

Straw, 1400 °C:

The size distribution of the original straw fuel presents a broad peak with maximum at ~400 µm. At the initial 0.25 s of conversion, this large-particle size peak decreases and tend to move towards slightly smaller particle sizes, which could indicate a certain degree of char fragmentation. SEM investigations of the 0.25s straw ash (Figure 6 a)) confirms that the sample contains numerous large, porous char particles, measuring up to >500 µm in diameter. The surface of some of the char particles appear partly melted, and more or less covered with smaller ash particles/droplets rich in Si.

At 1.0s residence time, the broad peak of large fuel/char particles originally positioned around ~400 µm is narrowed and shifted towards significantly larger particle sizes (~600 µm). The relative increase in particle size is different than seen for wood combustion, and it may suggest agglomeration of char/ash particles, probably initiated by softening/melting of the alkali-rich ash minerals. SEM investigations of the 1.0s straw ash (Figure 6 b)), however, show no clear evidence of agglomeration. Two characteristic, large (~500-600 µm long) particles covered with numerous tiny, KCl-rich particles (which lights up in the BSE image) are seen in the right-hand side of the picture. This suggests coalescence of ash droplets on receding char surfaces. The content of organic matter in the 1.0s straw ash is still significant (68 %, see Table 3), emphasizing that char particles may (still) be the largest contributor to the large-particle size mode positioned at ~600 µm. Besides the suggested possible agglomeration, the apparent shift towards larger particles, as compared to the initial fuel PSD, may simply reflect the relatively faster conversion of the lower fuel particle sizes as compared to the larger particles.

Also in consistence with the particle size distribution observed for wood ash, a new, intermediate size peak with maximum around 45 µm develops with increasing residence time/degree of straw conversion. SEM/EDS investigations of the 1.0s and 1.7s straw ash (Figure 6 b) and c)) reveal that the particles in the intermediate size interval from around 10 – 100 µm is predominantly a mix of spherical or irregular fly ash particles rich in Si and K, char fragments, and aggregates of submicron (aerosol) particles composed largely of KCl. The aggregates of submicron aerosols are often (partly) covering the fly ash and char particles.

As was also the case with PSD of wood ash, a third, submicron (vaporization-mode) peak in the size interval 0.1 – 1 µm also appears for straw ash (Figure 4), reflecting the presence of aerosol particles originating mainly from homogeneous nucleation and subsequent coagulation of flame-volatilized inorganic species (Vejahati et al., 2010). Again, this probably reflects that the aerosol particles originally present as agglomerates have been re-dispersed.

The tendencies seem to be consistent for straw cyclone ash converted at 1200 ^{o}C.

Quantification of release:

Ash and elemental mass balances were established for all experiments, according to the method described in equation (1) and (2). For each experiment, and throughout the fuels, the ash mass balance ($ή_{recov,ash}$) generally closed at > 43 wt% recovery, as indicated for selected wood and straw experiments in Table 3. Less than 100 % recovery rates indicates a general loss of particles – most probably due to ash deposition on the reactor walls. The corresponding elemental recovery ($ή_{recov,element}$) generally varied between 80 – 180% for K, 100 – 210 % for Cl, 35 – 145 % for S, and 45 – 150 % for Ca/Si, with a few lower or higher outliners.

The elemental release of K, Cl and S is plotted as a function of residence time in Figure 7, using the two quantification methods described in equations (3) and (4). The values for water soluble fractions of K, Cl and S, $ή_{w,,}$ used in the release quantification calculations are provided in Table 4. The release of Ca and Si was also quantified (by Method 1), and found to be generally less than 5 - 10 % (results not shown), confirming that it is sound to use (the average of) Ca and Si recovery % as basis for the elemental mass balance calculations (“stable marker elements” assumption) when using Method 2.

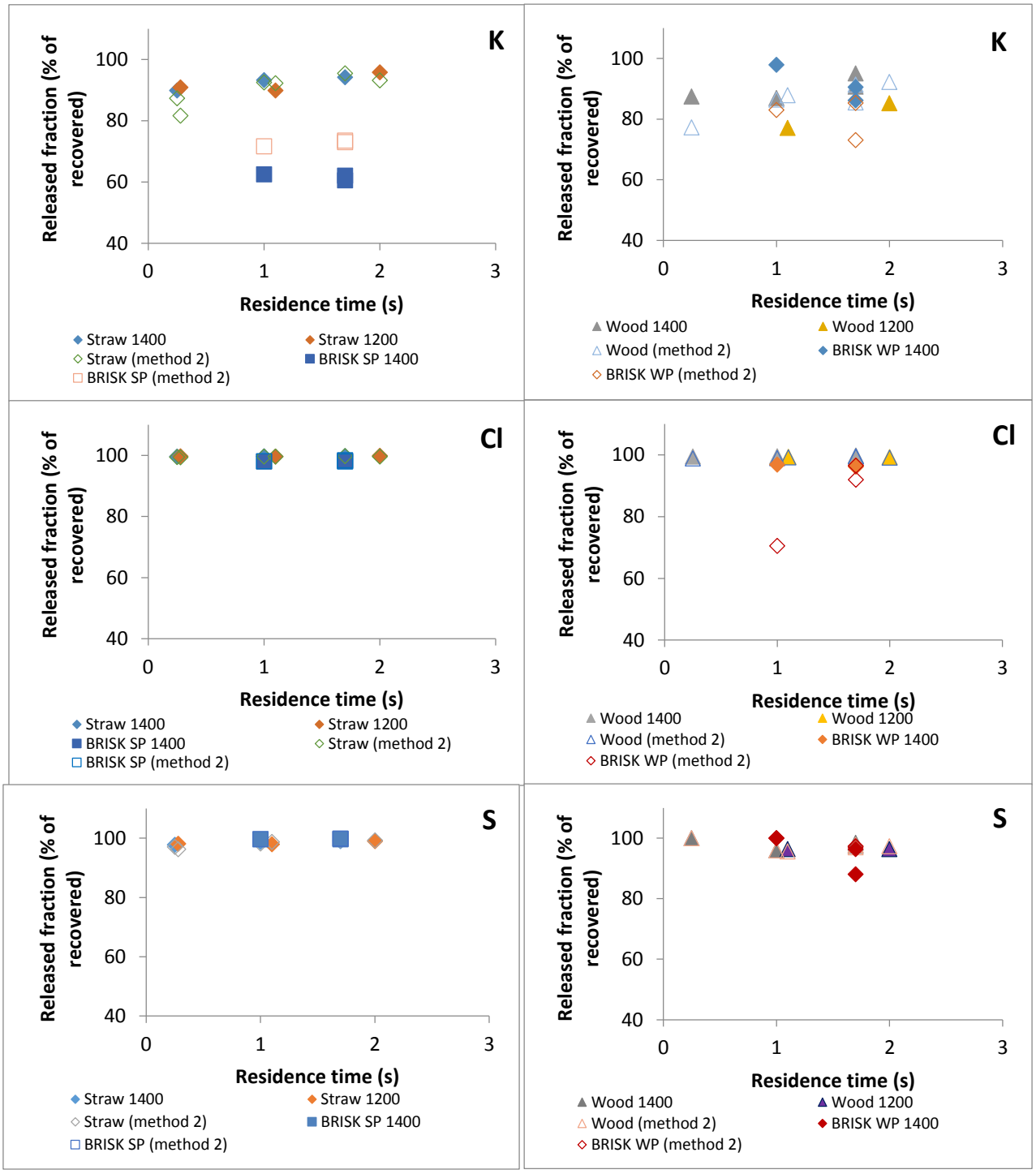

Figure 7: Release of K, Cl and S vs. residence time, as quantified by two methods. Left: straw fuels. Right: wood fuels

Table 4. Water soluble fractions, $ή_w$,, of K, Cl and S determined in cyclone ash for each fuel (average of several measurements).

		Straw	Wood	BRISK SP	BRISK WP
Water soluble fraction in cyclone ash ($ή_w$)	K	0.8	0.7	0.4	0.8
	Cl	0.99	0.99	0.95	(0.95)[1)]
	S	0.95	0.90	0.99	0.90

[1)] Estimated value (analytical data uncertain, as some values are below detection limit)

Figure 7 reveals that the release of K is large (> 60 wt.%) throughout the tested fuel range and residence times, though with some noticeable differences between the fuels. Depending on the quantification method used, the release of K from the studied fuels (except BRISK SP) amounts to 80 – 98 wt%, with a slight increasing trend with increasing residence time and/or temperature. A significantly lower release from "BRISK SP", as compared with the other studied fuels, is observed. This may be attributed to differences in mineral matter compositions between the fuels, such as levels of silicon relative to K and Ca (see Table 1). According to the definition by Knudsen (2004), "BRISK SP" is a Si-rich fuel ((K/Si) = 0.5), with relative shortage of Ca: ((K+Si)/(Ca+Mg) = 5.2), and as such retaining effects of silicates on the release of K may be expected, due to incorporation of K into silicate structures. The general massive release of K already at the initial 0.25 – 0.28s of conversion is in good agreement with the results obtained by Korbee et al. (2010), who found in their experiments that the alkali metals appeared to be vaporizing after about 90 ms of conversion.

The release of Cl is generally close to complete (except for BRISK WP, method 2), and independent of residence time and temperature. It should be noticed that when using quantification method 1, gaseous HCl is ignored (as it was not measured), and thus not included in the mass balance calculations. This may bias the results. The release obtained by method 2, however, is comparable, except for BRISK WP which exhibit a somehow lower release (≥ 70 %) when quantified by method 2. This may be attributed to very low concentrations of Cl in the analyzed ash fractions (close to detection limit), giving rise to large uncertainties on the results.
The release of S exhibits similar trends as for release of Cl. I.e. with the exception of "BRISK WP", which exhibits fluctuating results, the release of S is generally > 90 % for all fuels, independent on residence time and temperature. It should be noticed that the SO_2 concentration measured in the flue gas from the probe was very low/insignificant throughout the experiments, indicating that SO_2 initially released to the gas phase may have reacted to form alkali sulfates and or Ca/Mg sulfates at the points of sampling (Shah et al., 2010).

Conclusions:

Ash transformations, such as char burn-out and physical size development of residual fly ash, and transient release of flame-volatilized inorganic species, were studied during the initial conversion stages (0.25 – 2.0 s) of suspension-firing of biomass. Combustion experiments were carried out with bio-dust (two wood fuels and two straw fuels) in an entrained flow reactor, simulating full-scale suspension-firing of biomass.

Based on our experimental observations, the following conclusions are drawn:

-The char burn-out level of the residual ash is both time dependent and highly fuel dependent. The two wood fuels studied reached lower degree of conversion in the first 1.0 – 1.1 s of the combustion process, as compared to the two straw fuels, indicating that physical fuel properties such as particle sizes and shape may affect the char reactivity more significantly than e.g. the ash content and chemical composition.

-The physical size distribution of the residual fly ash particles evolves with residence time, towards a multi-modal particle size distribution. For wood, the particles shifts towards smaller particles with increasing time, due to char oxidation/pyrolysis, fragmentation, and ash formation, and there is no significant influence of ash melting. For straw, with 0.25 – 0.28 s of conversion, the PSD shifts slightly to smaller particles, due to devolatilization and char formation/fragmentation. At 1.0 – 2.0 s, the PSD shifts to larger particles, indicating melting and agglomeration of ash particles. With increasing time, the concentration of smaller particles also increases, due to char oxidation and char/ash fragmentation.

- The transient release of K is high for all fuels and throughout the temperature range tested. An increasing trend with increasing residence time indicate that the release of K is a time dependent process. For a Si-rich straw fuel with relatively shortage of Ca, results further indicate retaining effects on the release of K, probably due to incorporation of K into silicate structures. The release of Cl and S is generally close to complete for all fuels, independent on residence time and temperature.

Based on the herein obtained results and the existing literature in the field, and we may suggest the major transformation routes and transformation processes for ash forming elements during biomass suspension-firing as outlined in figure 8.

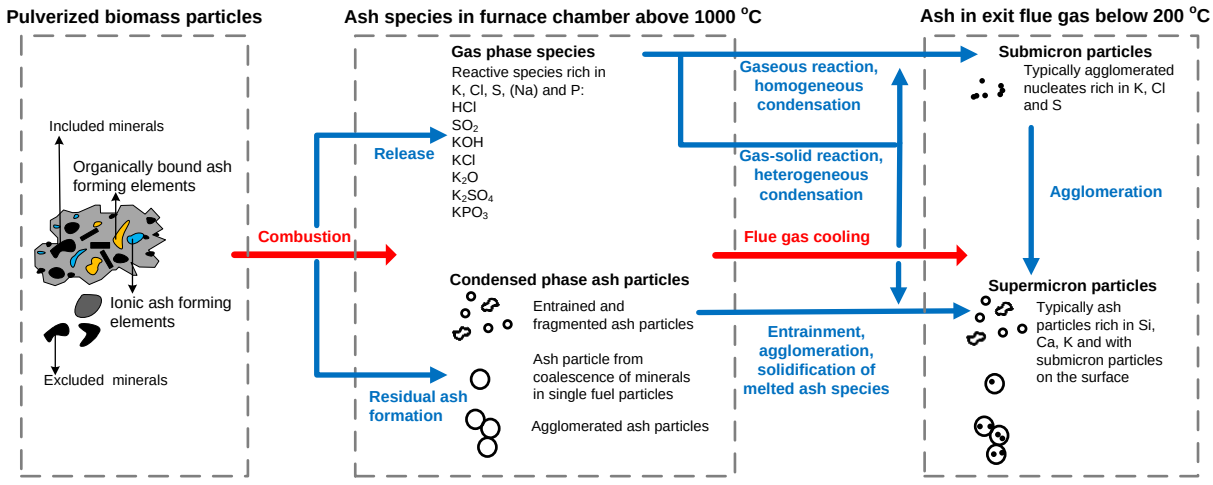

Figure 8. Major transformation routes and transformation processes for ash forming elements during biomass suspension-firing.

Acknowledgements
The work was funded by the Danish Strategic Research Center for Power generation from Renewable Energy (GREEN), and The European Research Infrastructure for Thermochemical Biomass Conversion (BRISK), and was carried out at the Combustion and harmful Emissions Control (CHEC) Research Centre, Department of Chemical and Biochemical Engineering, Technical University of Denmark.

References:

A. J. Damoe, H. Wu, F. J. Frandsen, P. Glarborg, B. Sander: Impact of Coal Fly Ash Addition on Combustion Aerosols (PM2.5) from Full-Scale Suspension-Firing of Pulverized Wood. Energy Fuels, 2014, 28, 3217−3223

The Danish Government. Our Future Energy; Danish Government: Denmark, 2011.
R. C. Flagan, J. H. Seinfeld: Fundamentals of Air Pollution Engineering. 1988.
F. J. Frandsen, S.C. van Lith, R. Korbee, P. Yrjas, R. Backman, I. Obernberger, T. Brunner, M. Jöller: Quantification of the release of inorganic elements from biofuels. Fuel Processing Technology 88 (2007) 1118 – 1128

S. B. Hansen, P. A. Jensen, F. J. Frandsen, H. Wu: Deposit probe measurements in large biomass-fired grate boilers and pulverized-fuel boilers. Energy & Fuels 28 (2014) 3539-3555

B. S. Haynes, M. Neville, R. J. Quann, A. F. Sarofim: Factors governing the surface enrichment of fly ash in volatile trace species. Journal of Colloid and Interface Science, Volume 87, Issue 1, May 1982, Pages 266–278

J. J. Helble: Mechanisms of ash particle formation and growth during pulverized coal combustion. Thesis (Ph. D.), Massachusetts Institute of Technology, Dept. of Chemical Engineering, 1987.

J.N. Knudsen: Volatilization of inorganic matter during combustion of annual biomass, Ph.D. Dissertation, Department of Chemical Engineering, Technical University of Denmark, Lyngby, 2004. ISBN: 87-91435-11-0

J.N. Knudsen, P.A. Jensen, W. Lin, K. Dam-Johansen: Secondary capture of chlorine and sulfur during thermal conversion of biomass, Energy & Fuels 2005, 19, 606-617

J.N. Knudsen, P.A. Jensen, K. Dam-Johansen: Transformation and release to the gas phase of Cl, K, and S during combustion of annual biomass, Energy & Fuels 2004, 18, 1385-1399

R. Korbee, K. V. Shah, M. Cieplik, C. I. Betrand, H. B. Vuthaluru, W. L. van de Kamp: First line transformations of coal and biomass fuels during pf combustion, Energy & Fuels 24, 897-909, 2010

A. Novaković , S.C. van Lith, F.J. Frandsen, P.A. Jensen, L.B. Holgersen: Release of potassium from the systems K-Ca-Si and K-Ca-P, Energy & Fuels, 2009, 23, 3423-3428

S. B. Saleh, J. P. Flensborg, T. K. Shoulaifar, Z. Sarossy, B. B. Hansen, H. Egsgaard, N. DeMartini, P. A. Jensen, P. Glarborg, K. Dam-Johansen: Release of Chlorine and Sulfur during Biomass Torrefaction and Pyrolysis. Energy Fuels, 2014, 28, 3738−3746

K.V. Shah, M.K. Cieplik, C.I. Bertrand, W.L. van de Kamp, H.B. Vuthaluru: Correlating the effects of ash elements and their association in the fuel matrix with the ash release during pulverized fuel combustion, Fuel Processing Technology 91 (2010) 531-545

S.C. van Lith: Release of inorganic elements during wood-firing on a grate, Ph.D. Dissertation, CHEC Research Center, Department of Chemical Engineering, Technical University of Denmark, 2005. ISBN: 87-91435-29-3

S.C. van Lith, V. Alonso-Ramírez, P.A. Jensen, F.J. Frandsen, P. Glarborg: Release to the gas phase of inorganic elements during wood combustion. Part 1: Development and evaluation of quantification methods, Energy & Fuels 2006, 20, 964-978

S.C. van Lith, P.A. Jensen, F.J. Frandsen, P. Glarborg: Release to the gas phase of inorganic elements during wood combustion. Part 2: Influence of fuel compostion, Energy & Fuels 2008, 22, 1598-1609

K. Qin, W. Lin, S. Fæster, P. A. Jensen, H. Wu, A. D. Jensen: Characterization of Residual Particulates from Biomass Entrained Flow Gasification. Energy Fuels (2013) 27, 262−270

F. Vejahati, Z. Xu, R. Gupta: Trace Elements in Coal: Associations with Coal and Minerals and Their Behavior during Coal Utilization-A Review. Fuel 89, 2010, 904–911.

H. Wu, P. Glarborg, F. J. Frandsen, K. Dam-Johansen, P. A. Jensen, B. Sander: Co-Combustion of Pulverized Coal and Solid Recovered Fuel In an Entrained Flow Reactor - General Combustion and Ash Behaviour. Fuel 90 (5), 2011, 1980-1991

Y. Zheng, P. A. Jensen, A. D. Jensen, B. Sander, H. Junker: Ash transformation during co-firing of coal and straw. Fuel 86 (2007) 1008-1020